

## Partial Transformation and the Two-Way Shape Recovery Characteristics

Wada K\*

College of Engineering, Swansea University, United Kingdom

### Abstract

It is widely known that two-way memory effect (TWME) is not an inherent property of shape memory alloy. The development of TWME requires thermomechanical training. Experimental study showed that undergoing partial reverse transformation in the course of training leads to the emergence of temporal two-step transformation, which was traditionally observed in the calorimetry measurement of an arrested stress-free heating cycle. The present work introduces a macromechanical approach to explain the mechanism of two-step transformation and its associated effects on stress-assisted two-way memory effect (SATWME) and TWME. The appearance of two-step transformation was observed to be a one-time only phenomenon and it clearly disappeared in the next full transformation. The disappearance of two-step transformation highlighted the occurrence of microstructural rearrangement driven by the internal stress field in the successive training cycles. A strain comparison demonstrated that the dominance of retransforming stress-assisted martensite (SAM) during cooling promoted the formation of internal back stress. This makes the accommodation process of deformation-induced martensite generated via pre-straining and SAM difficult, owing to which immobilizes the dislocations movement in the forward transformation direction, and causes detrimental effect on the TWME.

**Keywords:** NiTi; Shape memory alloy; Two-way memory effect (TWME); Partial transformation

### Introduction

#### Shape memory alloy

Since the first discovery of shape memory effect in a binary alloy of NiTi [1], the popularity of adopting shape memory alloy (SMA) has boosted rapidly in the vast area of medical and non-medical applications. It has been discovered that NiTi SMA is highly biocompatible, non-toxic, lightweight having distinctive advantage in strength to weight ratio, and capable of generating large excitation forces and displacements [2-5].

#### Two-way memory effect

The early 1970s experiments saw the clear evidence of reversible shape memory effect [6,7]. This effect is due to preferentially oriented martensite variants that are formed during cooling and revert to the austenite matrix during heating. The temperature changes are accompanied by the spontaneous macroscopic shape change. Alternatively, this reversible shape memory phenomenon was termed, two-way shape-memory effect (TWSME) [8]. Since then it has become common practice in a scientific community to adopt the abbreviation TWSME or simply TWME to describe such shape memory behavior. Because TWME is not an inherent property of SMA, it requires thermomechanical treatment often termed 'training' [9,10]. Another two-way shape memory behavior, stress-assisted two-way memory effect (SATWME) can be developed during the course of training procedure where a specimen is subjected to constrained thermal cycling.

#### Mechanism of TWME

When dealing with the underlying mechanism of TWME, it is essential to understand the macromechanical correlation between plastic strain and/or locally stabilized martensite level of the trained specimen and the subsequent magnitude of TWME. The generation of dislocations associated with the incomplete hysteresis of SATWME represents a prerequisite for generating TWME of high magnitude [11]. Also, for a training procedure involving martensite deformation and

stress-free cycling, the maximum TWME is achieved at certain pre-strain level where generation of plastic strain [12] and dislocations [13] are believed to be at optimum. The excessive plastic strain introduced as a result of partial reverse transformation is found to decrease the magnitude of TWME [14].

In this paper the proposed strain comparison approach unfolds the effects of partial transformation on SATWME and TWME by not only considering the progress in martensite deformation and its associated accommodation of stress-assisted martensite and deformation-induced martensite, but also the generation of forward and backward internal stresses.

### Experimental Setup and Procedures

#### Experimental apparatus

The specimens used in this work are near equiatomic NiTi wire with diameter = 0.185 mm. The wires were supplied by Nitinol Devices and Components, USA. As-received specimens were annealed at 580°C for 30 min in air, followed by air-cooling to room temperature. The transformation temperatures of as-annealed specimen were determined by differential scanning calorimetry (DSC, TA Instruments MDSC 2920). Pre-straining and thermomechanical cycling were all carried out using an Instron microforce testing system. Further details are described elsewhere [15].

#### Analysis procedures

Figure 1 shows the example of fully and partially transformed strain-temperature curves generated after 18% pre-strain and 200

\*Corresponding author: Wada K, College of Engineering, Swansea University, Bay Campus, Crymlyn Burrows, Swansea SA1 8EN, United Kingdom, Tel.: 441792606270; E-mail: [k.wada@swansea.ac.uk](mailto:k.wada@swansea.ac.uk)

Received May 19, 2016; Accepted June 01, 2016; Published June 11, 2016

Citation: Wada K (2016) Partial Transformation and the Two-Way Shape Recovery Characteristics. J Material Sci Eng 5: 262. doi:10.4172/2169-0022.1000262

Copyright: © 2016 Wada K. This is an open-access article distributed under the terms of the Creative Commons Attribution License, which permits unrestricted use, distribution, and reproduction in any medium, provided the original author and source are credited.

MPa cycling. The partial reverse transformation process was carried out by interrupting the course of reverse transformation at  $T_H$  (located between austenite start  $A_s$  and finish  $A_f$  temperatures), and immediately revert to below martensite finish  $M_f$  temperature by cooling. To study the characteristic of two-step transformation, the recovery strain generated in the first and second half of reverse transformation namely  $\epsilon_{R1}$  and  $\epsilon_{R2}$ , respectively (Figure 1b), were given comparison with the partially transformed strain,  $\epsilon_{PT}$ , and untransformed strain,  $\epsilon_{RM}$  (Figure 1a). This leads to the strain comparison plot, which will be presented in the next section.

In line with previous study [16], the deformation-induced martensite variants (generated via pre-straining) were classified as originally transformable martensite (ORT-M). From the partial reverse transformation point of view, the ORT-M corresponds to the fraction of retained martensite measured in terms of strain,  $\epsilon_{RM}$  (Figure 1a). Likewise, the stress-assisted martensite generated under constraint has been classified as primary transformed martensite (PRT-M). The PRT-M corresponds to a strain recovery evoked between  $M_s$  and  $M_f$  during 1<sup>st</sup> cooling. The characteristic of dislocations generation and microstructural anisotropy will be analyzed qualitatively by monitoring the slope changes in strain-temperature curve. Noticeably, the reference slope on 1<sup>st</sup> cooling modifies greatly

due to partial reverse transformation as shown in Figure 1a. In effect, with reference to full transformation, the change in  $M_s$  indicates development of internal stress due to dislocations generation, whereas the prolonged temperature interval,  $\Delta M = M_s - M_f$ , indicates pronounced microstructural anisotropy [17]. Wang and coworkers [18] also proposes that undergoing partial transformation is equivalent to imposing partial shear movements to bring the atomic arrangement to a state of confusion, i.e., anisotropy.

## Results and Discussion

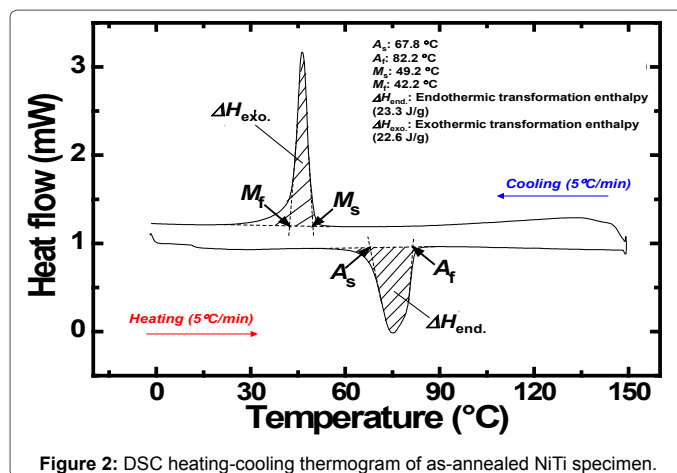
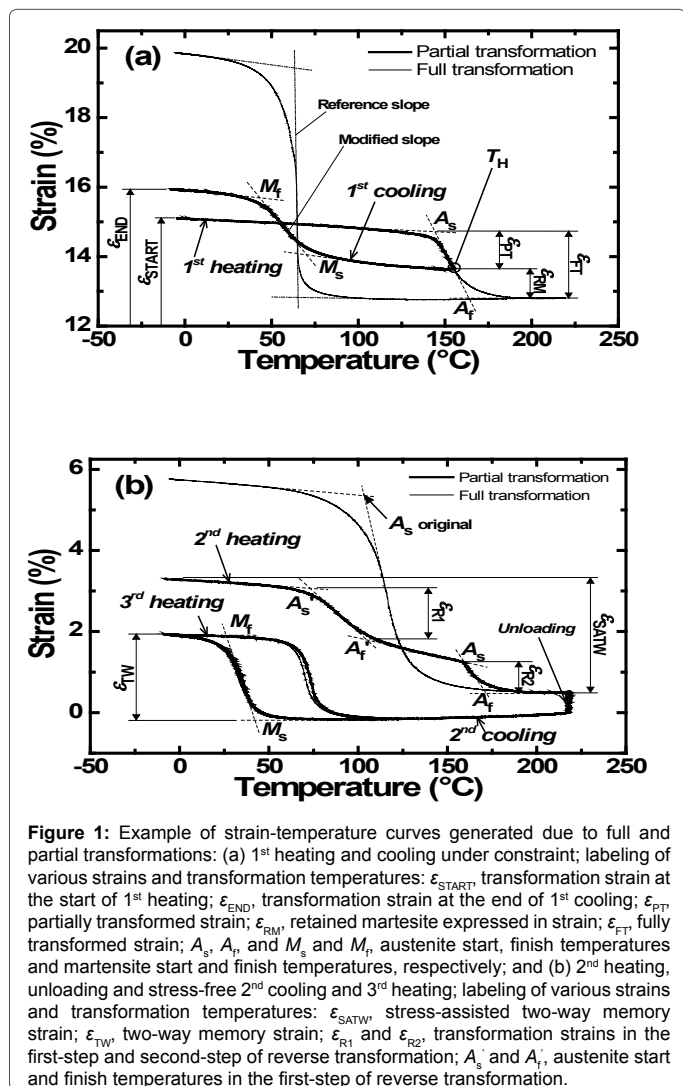
### As-annealed transformation temperatures

Thermally-induced transformation by and large is characterized by four temperatures:  $A_s$  and  $A_f$  during heating, and  $M_s$  and  $M_f$  during cooling.  $A_s$  and  $A_f$  indicate the temperatures at which the reverse transformation starts and finishes, whereas  $M_s$  and  $M_f$  indicate the temperatures at which transformation from parent phase (austenite) starts and finishes, respectively. Transformation temperatures at zero stress were determined by differential scanning calorimetry (DSC). The results are shown in Figure 2. Considering the  $M_f$ -temperature (42.2°C), it is apparent that the as-annealed specimens were in the fully martensitic state when deformed in tension at room temperature (approximately 20°C).

### Strain comparisons

The strain comparisons were made for the thermomechanical training condition: as-annealed NiTi specimen subjected to 4% pre-strain, followed by 50, 200 and 350 MPa constraint cycling. Figure 3 shows the stress-strain response of the specimen subjected to 4% pre-strain, unloaded and reloaded to the aforementioned 50, 200 and 350 MPa stress levels. The percentage of retained martensite was estimated by the strain ratio  $(\epsilon_{RM}/\epsilon_{FT}) \times 100\%$ . Based on the comparison plot produced for each of the conditions, a number of microscopic issues related to the macroscopic responses of SATWME and TWME are outlined.

Figure 4a shows the strain comparison plot for the case of 4% pre-strain with 50 MPa cycling. It can be seen that both  $\epsilon_{R1}$  and  $\epsilon_{R2}$  curves stayed in close proximity with their respective reference curves namely  $\epsilon_{PT}$  and  $\epsilon_{RM}$ . The close overlapping of  $\epsilon_{R2}$  and  $\epsilon_{RM}$  curves indicate the fact that the second half of reverse transformation (occurring between  $A_s$  and  $A_f$  in the 2<sup>nd</sup> heating, Figure 1b correspond to retained ORT-M transforming into austenite. A similar phenomenon is also observed under 200 and 350 MPa cycling as shown in Figures 4b and 4c,



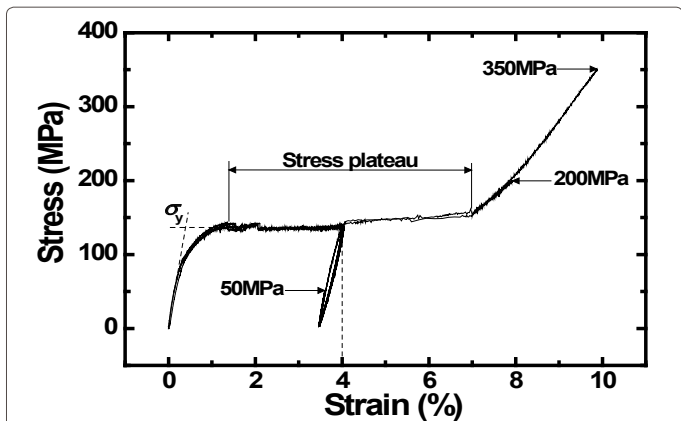


Figure 3: Stress-strain curves obtained at room temperature for the as-annealed NiTi specimens (loading, unloading and reloading to 50, 200 and 350 MPa).

respectively.

### Effect of partial transformation on SATWME

The insignificant difference observed between  $\epsilon_{R1}$  and  $\epsilon_{PT}$  curves under 50 MPa (Figure 4a) implies that the value of  $\epsilon_{SATW}$  is extremely insensitive to partial reverse transformation. This implication can be elaborated as follows: considering that applied constrained stress was relatively weak in directing the growth of stress-assisted martensite variants, and for this reason, the volume fraction of PRT-M generated would be small. In contrast, the volume fraction of PRT-M would proliferate with increasing magnitude of constrained stress, hence the value of  $\epsilon_{R1}$  gets larger than that of  $\epsilon_{PT}$  when subjected to 200 and 350 MPa (Figures 4b and 4c). These PRT-M variants are required to accommodate themselves with the neighboring retained ORT-M variants in the 1<sup>st</sup> cooling following the 1<sup>st</sup> heating of partial reverse transformation. The orientation mismatch among ORT-M and PRT-M variants causes internal plastic deformation as a means of coordination mechanism. The consequence is reflected by the separation of the two austenite start-finish peaks,  $A_s-A_f'$  [15]. Linking the experimental observations of  $A_s-A_f'$  to the present strain comparison plot, it is possible that the acute decrease of  $\epsilon_{R1}$  observed at low %RM level is caused by a higher degree of internal plastic deformation. For the case of 50 MPa, the adverse effect of this plastic deformation on  $\epsilon_{SATW}$  is suppressed with increasing %RM, possibly due to a localized martensite deformation behavior. As shown in Figure 3, the martensite deformation process was terminated in the midst of partial detwinning region (stress plateau). On a microscopic scale, some fraction of the martensite variants experience higher deformation than the applied pre-strain, while others experience lesser deformation to alleviate the plastic deformation.

### Effect of partial transformation on TWME

Experimentally, it was suggested that the magnitude of TWME depends on the dislocation structures produced by training [15]. This is related to a characteristic arrangement of dislocations and the density of dislocations produced thereby [19,20]. In fact, the aligned dislocations distributed uniformly inside martensite are regarded as the main characteristic feature of post-trained specimen exhibiting TWME [21].

It is proposed by the present author that the introduction of retained martensite (ORT-M) disrupts these aligned dislocations arrangement to be heterogeneous and lowers the TWME. To what extent the presence

of disrupted dislocations impinge on the TWME is being investigated by observing the shift of equal strain position, defined by  $\Delta ESP = ESP_f - ESP_i$ , and its related phenomena. The amount of shift and its direction are denoted by the bold dashed line with a closed arrow-head (Figure 4). Apparently, the initial equal strain position,  $ESP_i$  is determined by the intersection of  $\epsilon_{PT}$  and  $\epsilon_{RM}$  curves; the symbol  $\epsilon_i$  has been assigned to represent the strain level at  $ESP_i$ . In the same way, the final equal strain position,  $ESP_f$  is determined by the intersection of  $\epsilon_{R1}$  and  $\epsilon_{R2}$  curves, and its associated strain level is the  $\epsilon_f$ . Thus, the shift of equal strain position will be accompanied by the shift of strain level,  $\Delta\epsilon = \epsilon_f - \epsilon_i$ .

Table 1 summarizes the quantification of these equal strain positions directly measured from Figure 4. Obviously, the position of  $ESP_i$  is located at near 50% RM irrespective of the training conditions, thus  $\Delta ESP = ESP_f - 50\%$ . The  $ESP_i$  shifts to a new position  $ESP_f$ , which is caused by the trend displayed in  $\epsilon_{R1}$  curve. As indicated by the positive

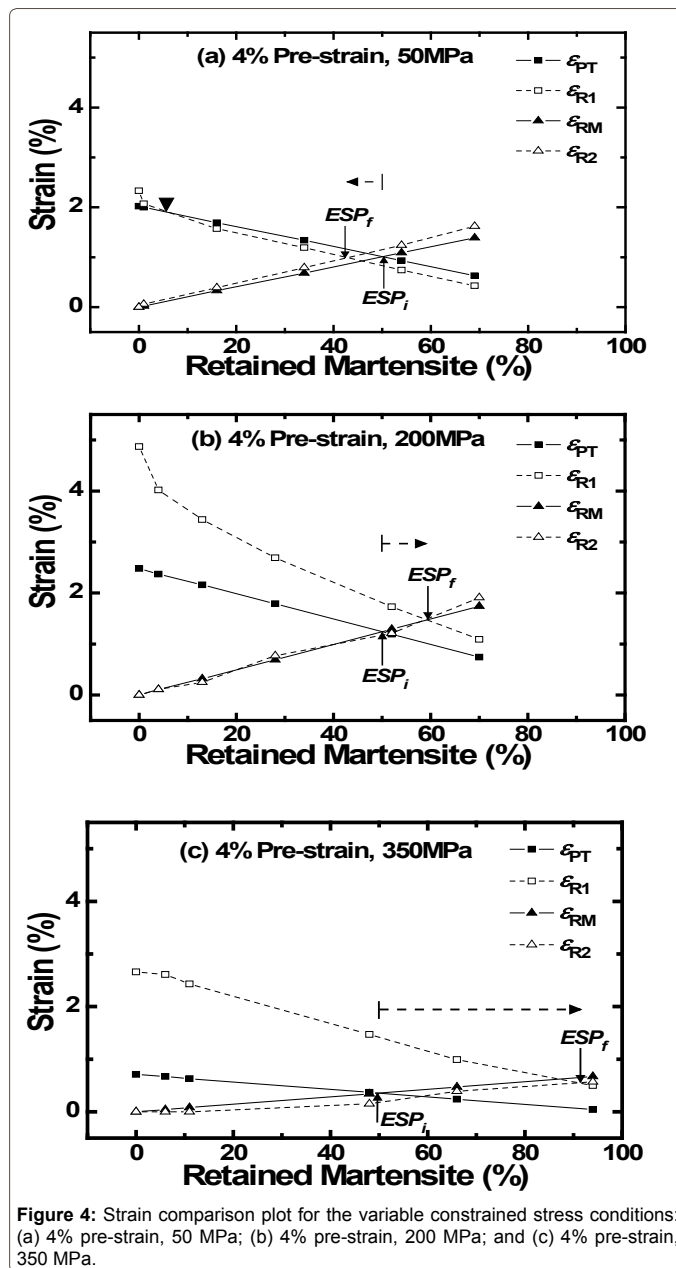


Figure 4: Strain comparison plot for the variable constrained stress conditions: (a) 4% pre-strain, 50 MPa; (b) 4% pre-strain, 200 MPa; and (c) 4% pre-strain, 350 MPa.

$\sigma$ (MPa)	ESP <sub>f</sub> (%)	$\Delta$ ESP (%)	$\epsilon_i$ (%)	$\epsilon_f$ (%)	$\Delta\epsilon$ (%)	Remark
50	42.9	-7.1	1.01	0.99	-0.02	ORT-M (deformation-induced martensite) dominant
200	59.0	9.0	1.24	1.48	0.24	PRT-M (stress-assisted martensite) dominant
350	91.1	41.1	0.36	0.55	0.19	Extremely PRT-M (stress-assisted martensite) dominant

\* $\Delta$ ESP = ESP<sub>f</sub> - 50%

**Table 1:** The shift of equal strain position (ESP) for the variable constrained stress conditions.

value of  $\Delta$ ESP, applying high constrained stress tends to make PRT-M dominant in the two-step reverse transformation. In other words the amount of recovery in  $\epsilon_{SATW}$  is dominated by the PRT-M variants transforming into austenite. Associated with the value of  $\Delta$ ESP, the dominance of PRT-M causes the  $\Delta\epsilon$  to be increased, though its increment is not directly proportional to the  $\Delta$ ESP.

The observed shift of ESP arises from the following repercussion: Olson et al. [22] observed that the nucleation of stress-assisted martensite (i.e., refers to PRT-M in the present investigation) do not engage in the creation of new sites or embryos by plastic deformation. Further observations by Sehitoglu et al. [23] have shown that the constrained cycling tend to favor the growth of selected variants in expense of others. Based on these observations, it can be suggested that PRT-M variants would persist on nucleating at their preferred sites without having to destroy the nucleation sites provided for the retained ORT-M during the 1<sup>st</sup> cooling. Obviously, this persistence of nucleating PRT-M is reflected by the ESP<sub>f</sub> shifting to a higher %RM level and is observed to be particularly prominent for the case of 350 MPa. This phenomenon occurs due to the fact that greater the magnitude of constrained stress the larger is the volume fraction of stress-assisted martensite produced [24]. In this respect, the opposite scenario of ESP<sub>f</sub> shifting to a lower %RM could indicate the arrest of PRT-M persisting to nucleate over ORT-M.

It is then anticipated that the heterogeneous dislocations will be formed in the microstructure when ORT-M and PRT-M variants try to coordinate with each other. It has been observed experimentally that the occurrence of contractive recovery on the stress-free 2<sup>nd</sup> cooling is the sign of intermediate R-phase (rhombohedral-phase) formation caused by the strong backward internal stress [15]. The formation of R-phase during the course of TWME is suggested to be imposed by heterogeneity in the local stress field, which is a direct consequence of changes in the dislocation configuration [25]. In this respect, it is possible to deduce higher degree of disrupted dislocations being produced for the ones with apparent R-phase or dominant backward internal stress formation.

**Effect of partial transformation on SATWME and TWME under repeated cycles**

Figure 5 shows the thermomechanical training cycles of as-annealed specimen subjected to 4% pre-strain and repeated four cycles under 200 MPa constrained stress, followed by stress-free cycling to induce TWME (denoted by  $\epsilon_{TW}$ ). The dominant forward internal stress, which is reflected by the progressive increase of  $M_s$  temperature, favors the development of TWME (Figure 5a). As shown in Table 2, the value of  $M_s$  temperature progressively increases with an increase in the number of cycles. In contrast, partial transformation in 1<sup>st</sup> heating induces two-step reverse transformation in the 2<sup>nd</sup> heating (Figure 5b),

Cyclic condition	M <sub>s</sub> temperature at the (N <sup>th</sup> ) number of cycle (°C)				Remark
	(1)	(2)	(3)	(4)	
Full transformation	67.32	70.26	71.77	72.46	Data extracted from Figure 5(a)
Partial transformation at 1 <sup>st</sup> heating (arrested at T <sub>H</sub> )	67.01	67.85	69.92	71.65	Data extracted from Figure 5(b)

**Table 2:** Effect of partial transformation on the M<sub>s</sub> temperature.

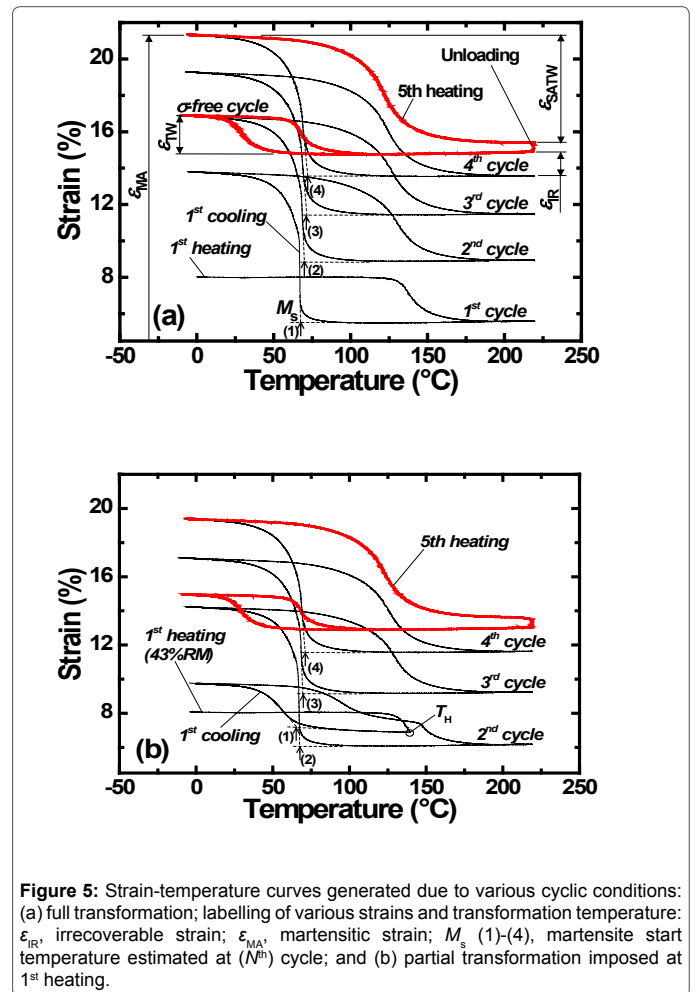


**Figure 5:** Strain-temperature curves generated due to various cyclic conditions: (a) full transformation; labelling of various strains and transformation temperature:  $\epsilon_{IR}$ , irrecoverable strain;  $\epsilon_{MA}$ , martensitic strain;  $M_s$  (1)-(4), martensite start temperature estimated at (N<sup>th</sup>) cycle; and (b) partial transformation imposed at 1<sup>st</sup> heating.

which disappears in the subsequent cycles. The disappearance of two-step transformation highlighted the occurrence of microstructural rearrangement (i.e., rearranging to repair the disruption caused by the accommodation of ORT-M and PRT-M variants) driven by the internal stress field in the successive training cycles. Evidently, there is an apparent and prominent rise in  $M_s$  temperature between the 2<sup>nd</sup> and 3<sup>rd</sup> cycle as shown in Table 2.

Table 3 summarizes the effect of partial transformation on SATWME and TWME. It can be seen that the magnitudes of  $\epsilon_{MA}$ ,  $\epsilon_{SATW}$  and  $\epsilon_{TW}$  all decreases due to partial transformation. The close match in the values of  $\Delta\epsilon_{IR}$  and  $\Delta\epsilon_{TW}$  implies that plastic strain introduced by the partial transformation directly removes the portion of recoverable strain in TWME. By following the same thought that disorderly distributed dislocations promote the removal of martensite variant participating in the spontaneous shape recovery [26], the magnitude of TWME decreases.

Cyclic condition	$\epsilon_{SATW}$ (%)	$\epsilon_{TW}$ (%)	$\Delta\epsilon_{TW}$ (%)	$\epsilon_{MA}$ (%)	$\epsilon_{IR}$ (%)	$\Delta\epsilon_{IR}$ (%)	Remark
Full transformation	5.95	2.14	-	21.35	1.34	-	Data extracted from Figure 5(a)
Partial transformation at 1 <sup>st</sup> heating (arrested at $T_H$ )	5.78	2.08	0.06	19.40	1.41	0.07	Data extracted from Figure 5(b)

Table 3: Effect of partial transformation on SATWME and TWME.

## Conclusions

The mechanism of two-step transformation due to partial transformation was further elucidated by the macromechanical approach. A strain comparison approach demonstrated that the generation of two-step transformation is proceeded by the sequential transformation of retransforming stress-assisted martensite (SAM) and retained deformation-induced martensite generated via pre-straining in the order of increasing temperature. The dominance of deformation-induced martensite and SAM with respect to varying amount of retained martensite (%RM) was analyzed by the shift of equal strain position. Whereas the dominance of SAM promoted the formation of backward internal stress causing severe impingement on the first half of reverse transformation ( $\epsilon_{R1}$ ), the dominance of deformation-induced martensite suppressed the decrease of  $\epsilon_{R1}$ .

The defects retained from the constrained thermal cycling gave rise to the simultaneous formation of forward and backward internal stresses, as reflected by the changes in  $M_s$  temperature. The former stress guides the martensite variant into preferred orientation, which led to the higher magnitudes of two-way shape recoveries. The latter stress makes the accommodation process of deformation-induced martensite and SAM difficult, owing to which immobilizes the dislocations movement in the forward transformation direction, and causes detrimental effect on the TWME.

## Acknowledgement

The author gratefully acknowledges the College of Engineering Swansea University financial support grants code number EGD115. Also expresses his sincere gratitude to Associate Professor Liu Yong from Nanyang Technological University for the past years' insightful guidance and mentoring support.

## References

- Buehler WJ, Gilfrich JV, Wiley RC (1963) Effect of Low-Temperature Phase Changes on the Mechanical Properties of Alloys near Composition TiNi. J Appl Phys 34: 1475-1477.
- Lecce L, Concilio A (2015) Shape Memory Alloy Engineering for Aerospace, Structural and Biomedical Applications. (1<sup>st</sup> Edn.), Elsevier, Netherlands.
- Van Humbeeck J (1999) Non-Medical Applications of Shape Memory Alloys. Mater Sci Eng A 275: 134-148.
- Duerig T, Pelton A, Stöckel D (1999) An Overview of Nitinol Medical Applications. Mater Sci Eng A 275: 149-160.
- Chopra I (2002) Review of State of Art of Smart Structures and Integrated Systems. AIAA J 40: 2145-2187.

- Nagasawa A, Enami K, Ishino Y, Abe Y, Nenno S (1974) Reversible Shape Memory Effect. Scripta Metall 8: 1055-1060.
- Saburi T, Nenno S (1974) Reversible Shape Memory Effect in Cu-Zn-Ga. Scripta Metall 8: 1363-1367.
- Tas H, Delaey L, Deruyttere A (1972) Stress-Induced Transformations and the Shape-Memory Effect. J Less-Common Met 28: 141-151.
- Duerig TW, Melton KN, Stöckel D, Wayman CM (1990) Engineering Aspects of Shape Memory Alloys. Butterworth-Heinemann Ltd, London.
- Wayman CM (1992) Shape Memory and Related Phenomena. Prog Mater Sci 36: 203-224.
- Scherngell H, Kneissl AC (2002) Generation, Development and Degradation of the Intrinsic Two-Way Shape Memory Effect in Different Alloy Systems. Acta Mater 50: 327-341.
- Airoldi G, Ranucci T, Riva G, Sciacca A (1996) The Two-Way Memory Effect by the Pre-Strain Training Method in a 50Ti40Ni10Cu (at.%) alloy. Scripta Mater 34: 287-292.
- Liu YN, Liu Y, Van Humbeeck J (1999) Two-Way Shape Memory Effect Developed by Martensite Deformation in NiTi. Acta Mater 47: 199-209.
- Wada K, Liu Y (2007) Thermomechanical Training and the Shape Recovery Characteristics of NiTi Alloys. Mater Sci Eng A 482: 166-169.
- Wada K, Liu Y (2007) On the Two-Way Shape Memory Behavior in NiTi Alloy-An Experimental Analysis. Acta Mater 56: 3266-3277.
- Wada K, Liu Y (2008) On the Mechanisms of Two-Way Memory Effect and Stress-Assisted Two-Way Memory Effect in NiTi Shape Memory Alloy. J Alloys Compd 449: 125-128.
- Guilemany JM, Gil FJ (1990) The Influence of Grain Boundaries on the Transformation Temperatures of Cu-Zn-Al Shape Memory Alloys. Mat Res Bull 25: 1325-1332.
- Wang FE, DeSavage BF, Buehler WJ, Hosler WR (1968) The Irreversible Critical Range in the TiNi Transition. J Appl Phys 39: 2166-2175.
- Kajiwara S, Kikuchi T (1982) Dislocation Structures Produced by Reverse Martensitic Transformation in a Cu-Zn Alloy. Acta Metall 30: 589-598.
- Rios-Jara D, Guenin G (1987) On the Characterization and Origin of the Dislocations Associated with the Two Way Memory Effect in Cu-Zn-Al Thermoelastic Alloys - I. Quantitative Analysis of the Dislocations. Acta Metall 35: 109-119.
- Zhu M, Chen FX, Yang DZ (1991) Microstructures of 18R Martensite Induced by Deformation and Thermomechanical Cycles in CuZnAl Shape Memory Alloy. J Mater Sci 26: 5527-5533.
- Olson GB, Cohen M (1972) A Mechanism for the Strain-induced Nucleation of Martensitic Transformations. J Less-Common Met 28: 107-118.
- Sehitoglu H, Karaman I, Zhang X, Viswanath A, Chumlyakov Y, et al. (2001) Strain-Temperature Behavior of NiTiCu Shape Memory Single Crystals. Acta Mater 49: 3621-3634.
- Hamilton RF, Sehitoglu H, Chumlyakov Y, Maier HJ (2004) Stress Dependence of the Hysteresis in Single Crystal NiTi Alloys. Acta Mater 52: 3383-3402.
- Chrobak D, Stroz D, Morawiec H (2003) Effect of Early Stages of Precipitation and Recovery on the Multi-Step Transformation in Deformed and Annealed Near-Equiatomic NiTi Alloy. Scripta Mater 48: 571-576.
- Bai YJ, Shi QQ, Sun DS, Bian XF, Geng GL (1999) Influence of Dislocation Structure on Two-Way Shape Memory Effect in a CuZnAlMnNi Alloy. J Mater Sci Lett 18: 1509-1511.